

FEM AND BEM ANALYSES OF NOTCH STRESS INTENSITY FACTORS IN ANISOTROPIC MATERIALS

M. Heinzlmann, M. Kuna and M. Busch \*

The asymptotic stress field at sharp notches in orthotropic materials can be described as the sum of one or two singularity terms, where the first term corresponds to symmetric and the second term to antisymmetric loading of the notch. Following Stroh's formalism, the stress exponents and angular functions have been calculated analytically for a notch in monocrystalline silicon between two (111) lattice planes. To calculate the notch stress intensity factors (NSIFs), which are a measure for the magnitude of the stress terms, the Finite Element Method (FEM) and the Boundary Element Method (BEM) have been employed. Using FEM, the NSIFs were extracted from the nodal stresses ahead of the notch tip. Using BEM, the NSIFs can be obtained directly by incorporating singular notch tip elements into the BEM code. Very good agreement was achieved for the NSIFs calculated by the two numerical techniques.

INTRODUCTION

For modern micromechanical components as sensors, actuators, micromachines etc., the problems of mechanical reliability, strength and material behaviour play an increasing role (Heuberger (1) and Petersen (2)). Micromechanical components are produced from monocrystalline silicon wafers employing the well known technologies from microelectronics, involving anisotropic etching techniques (1), (2). As a consequence of these etching processes, nearly atomically sharp notches occur in the structures, which are frequently the origin of failure of the structures by brittle fracture. The reason is the stress concentration at the notches under mechanical or thermal loading. Therefore, an assessment of the reliability of a notched structure requires the knowledge of the notch tip stress field.

THE NOTCH TIP STRESS FIELD

The notch tip stress field in arbitrarily anisotropic materials can be described by a power series expansion where the stress exponents and angular functions can be calculated analytically with the Stroh formalism (3,4), as will be outlined in the following.

\* Fraunhofer-Institut für Werkstoffmechanik, Aussenstelle Halle, Heideallee 19, D-06120 Halle, Germany

Within linear elasticity, the displacement-strain relation, the equilibrium equation, and the stress-strain relation of any material are expressed by

$$\epsilon_{ks} = \frac{1}{2}(u_{k,s} + u_{s,k}) \quad (1),$$

$$\sigma_{ij} = c_{ijks}\epsilon_{ks} \quad (2),$$

$$\text{and } \sigma_{ij,j} = 0 \quad (3),$$

where  $u_k$  is the displacement vector,  $\sigma_{ij}$  and  $\epsilon_{ks}$  are the stress and strain tensor and  $c_{ijks}$  is the elasticity tensor, respectively. Assuming the displacement field  $u_k$  is independent of the cartesian coordinate  $x_3$ ,  $u_k$  can be written as

$$u_k = a_k f(Z) \quad (4)$$

with

$$Z = r(\cos \varphi + p \sin \varphi) \quad (5)$$

in polar coordinates, where the complex number  $p$  is an eigenvalue and  $a_k$  the corresponding eigenvector found from the elasticity constants. Substituting eq.s (1) - (3) into eq. (4), we obtain

$$(c_{i1k1} + p(c_{i1k2} + c_{i2k1}) + p^2 c_{i2k2})a_k = 0 \quad (6),$$

which results in a nontrivial solution for  $a_k$  only if the determinant of the matrix vanishes. For orthotropic materials, the vanishing of the determinant means

$$\begin{vmatrix} c_{1111} + p^2 c_{1212} & p(c_{1122} + c_{1212}) & 0 \\ p(c_{1122} + c_{1212}) & c_{1212} + p^2 c_{2222} & 0 \\ 0 & 0 & c_{1313} + p^2 c_{2323} \end{vmatrix} = 0 \quad (7).$$

Hence, eq. (6) leads to a quadratic and a quartic equation in  $p$ . As was shown by Ting and Chou (5), the two solutions of the quadratic equation correspond to anti-plane deformation, whereas the four solutions of the quartic equation correspond to in-plane deformation. It can be shown (3) that for a positive strain energy, the solutions for  $p$  cannot be real. Thus, the six solutions  $p_{(\omega)}$  are three pairs of complex conjugate numbers. Having calculated  $p_{(\omega)}$  from eq. (7) and  $a_{k(\omega)}$  from eq. (6), the stresses pertaining to each eigenvalue are obtained with eq.s (1), (2) and (4), and can be superimposed linearly to give

$$\sigma_{ij} = \sum_{\omega=1}^4 x_{(\omega)} (c_{ijk1} + p_{(\omega)} c_{ijk2}) a_{k(\omega)} \frac{d}{dZ_{(\omega)}} f(Z_{(\omega)}) \quad (8)$$

for stress terms pertaining to in-plane deformation. To determine the exponents  $\lambda$  of the series expansion of the notch tip stress field, let  $f(Z)$  be chosen as

$$f(Z) = \frac{Z^{1-\lambda}}{1-\lambda} \quad (9).$$

Substituting eq. (9) into eq. (8) and applying the boundary conditions of stress-free notch faces leads to the eigenvalue equation

$$D_{\mu\omega}x_{\omega} = 0 \quad (10),$$

where the eigenvector  $x_{\omega}$  corresponds to the coefficients in eq. (8) and the  $4 \times 4$  matrix  $D_{\mu\omega}$  is given with eq.s (5), (8) and (9) as

$$D_{\mu\omega} = (c_{\mu 2k1} + p_{(\omega)}c_{\mu 2k2})a_{k(\omega)}(\cos \varphi_1 + p_{(\omega)} \sin \varphi_1)^{1-\lambda} \quad (11a)$$

$$\text{and } D_{\mu\omega} = (c_{(\mu-2)2k1} + p_{(\omega)}c_{(\mu-2)2k2})a_{k(\omega)}(\cos \varphi_2 + p_{(\omega)} \sin \varphi_2)^{1-\lambda} \quad (11b)$$

for  $\mu=1,2$  (eq. 11a) and  $\mu=2,3$  (eq. 11b), respectively. In eq. (11),  $\varphi_1$  and  $\varphi_2$  are the polar angles of the notch faces. With eq. (10),  $\lambda$  is obtained as the eigenvalue for which the determinant of  $D_{\mu\omega}$  vanishes.

Eq. (8) can be rewritten in a more convenient form as

$$\sigma_{ij(n)}(r, \varphi) = A_{(n)} \cdot f_{ij(n)}(\varphi) \cdot r^{-\lambda_{(n)}} \quad (12),$$

where the eigenvalue  $\lambda_{(n)}$  is the stress exponent and  $f_{ij(n)}(\varphi)$  are angular functions. Stress terms with  $\lambda_{(n)} > 0$  are singular. The angular functions  $f_{ij(n)}(\varphi)$  can be calculated analytically from the eigenvector  $x_{\omega}$  with eq.s (5), (6) and (9) by normalizing the components of the eigenvector such that  $f_{\varphi\varphi}(\varphi=0)=1$  for stress terms pertaining to symmetric loading of the notch and  $f_{r\varphi}(\varphi=0)=1$  for stress terms pertaining to anti-symmetric loading of the notch, where  $\varphi=0$  is the polar angle of the ligament ahead of the notch tip. The notch stress intensity factor (NSIF)  $A_{(n)}$ , which then uniquely determines the stress term, depends on the geometry and loading of the whole structure and has to be calculated numerically. Note that the dimension of  $A$ ,  $MPa \cdot m^{\lambda}$ , depends on the magnitude of the stress exponent  $\lambda$ .

#### DETERMINATION OF THE STRESS FIELD PARAMETERS FOR MONO-CRYSTALLINE SILICON STRUCTURES

With the equations of the previous chapter, the stress exponents  $\lambda$  and the angular functions  $f_{ij}(\varphi)$  can be determined analytically for anisotropic materials. For monocrystalline silicon in the  $(x_1, x_2, x_3)$  coordinate system of the notched plate investigated in the following chapter, the elasticity tensor  $c_{ijkl}$  consists of the nonzero components  $c_{1111}=1,6564 \cdot 10^{11} \text{Pa}$ ,  $c_{2222}=c_{3333}=1,943 \cdot 10^{11} \text{Pa}$ ,  $c_{1122}=c_{1133}=0,6394 \cdot 10^{11} \text{Pa}$ ,  $c_{2233}=0,3528 \cdot 10^{11} \text{Pa}$ ,  $c_{2323}=0,5085 \cdot 10^{11} \text{Pa}$  and  $c_{1313}=c_{1212}=0,7951 \cdot 10^{11} \text{Pa}$ . For a notch between two (111) lattice planes with an opening angle of  $70,52^\circ$ , this leads to the two singular stress exponents

$$\lambda_1 = 0,4814 \quad \text{and} \quad \lambda_2 = 0,2392 \quad (13),$$

where  $\lambda_1$  pertains to symmetric (mode 1) loading, and  $\lambda_2$  to anti-symmetric (mode 2) loading of the notch. Hence, the notch tip stress field can be described by

$$\sigma_{ij}(r, \varphi) = A_1 f_{ij1}(\varphi) r^{-\lambda_1} + A_2 f_{ij2}(\varphi) r^{-\lambda_2} \quad (14).$$

The angular functions  $f_{\varphi\varphi 1}(\varphi)$ ,  $f_{r\varphi 1}(\varphi)$ ,  $f_{\varphi\varphi 2}(\varphi)$  and  $f_{r\varphi 2}(\varphi)$  are plotted in fig.s 1 and 2.

To calculate the NSIFs  $A_{(n)}$ , numerical methods, e.g. the Finite Element Method (FEM) or the Boundary Element Method (BEM), have to be used. Since singular finite elements for V-notches exist so far only for isotropic materials (Lin and Pin Tong (6)), the FEM determination of the NSIFs in anisotropic materials is based on the nodal stresses around the notch tip. This requires a particularly fine mesh around the notch tip, see fig. 3, showing the FEM mesh of a notched plate. To determine both  $A_1$  and  $A_2$  from the nodal stresses, it is necessary to distinguish between the contribution of the first and second stress term to the nodal stresses. The angular functions  $f_{\varphi\varphi}(\varphi)$  and  $f_{r\varphi}(\varphi)$  (see fig.s 1 and 2) show that along  $\varphi=0$ ,  $\sigma_{r\varphi}$  vanishes for the first stress term, and  $\sigma_{\varphi\varphi}$  vanishes for the second stress term. It is therefore convenient to determine  $A_1$  from  $\sigma_{\varphi\varphi}$  and  $A_2$  from  $\sigma_{r\varphi}$  along  $\varphi=0$ . Fig. 5 shows a  $\log(\sigma_{\varphi\varphi})$  and  $\log(\sigma_{r\varphi})$  vs.  $\log(r)$  plot along  $\varphi=0$ . Linear dependences of  $\log(\sigma_{\varphi\varphi})$  and  $\log(\sigma_{r\varphi})$  on  $\log(r)$  are obtained in the vicinity of the notch tip. The slopes of the lines are  $\lambda_1$  and  $\lambda_2$ , respectively, and  $A_1$  and  $A_2$  can be determined from the location of the corresponding line with eq. (14).

The Boundary Element Method provides a somewhat more elegant way to calculate the NSIFs. Besides the general advantage that only the boundary of the notched structure has to be modelled, the stress singularities can easily be modelled with special notch tip elements that incorporate shape functions with the appropriate  $r^{-\lambda}$  stress singularities. This technique has already successfully been applied to handle crack tip singularities (Busch (7)). Therefore, a BEM mesh of a notched structure may be significantly coarser around the notch tip, see fig. 4.

### NUMERICAL RESULTS

For the notched plate shown in fig.s 3 and 4 (plate height: 10mm, plate width: 5mm, notch depth: 2.5mm, notch opening angle:  $70,52^\circ$ ), the NSIFs have been calculated by FEM and BEM for three different load cases. In all load cases, the bottom side of the plate was rigidly fixed and the plates were loaded by prescribing a common displacement to the nodes at the top side of the plate. The prescribed displacements in horizontal (u) and vertical (v) direction were  $u=0$  and  $v=10^{-3}$ mm in load case 1,  $u=10^{-3}$ mm and  $v=0$  in load case 2, and  $u=v=10^{-3}$ mm in load case 3. Thus, load case 1 corresponds to pure symmetric loading, load case 2 to pure anti-symmetric loading, and load case 3 to combined symmetric and anti-symmetric loading. The NSIFs calculated by FEM and BEM agree excellently, see table 1.

TABLE 1 - NSIFs calculated by FEM and BEM for the three different load cases.

load case	$A_{1-FEM}$ [MPa m <sup>0,4814</sup> ]	$A_{2-FEM}$ [MPa m <sup>0,2392</sup> ]	$A_{1-BEM}$ [MPa m <sup>0,4814</sup> ]	$A_{2-BEM}$ [MPa m <sup>0,2392</sup> ]
1	0,632	0	0,638	0
2	0	1,178	0	1,159
3	0,632	1,178	0,638	1,159

SUMMARY AND CONCLUSIONS

For the example of notches between two (111) lattice planes in monocrystalline silicon, the stress exponents and angular functions of the singular stress fields were calculated analytically. The stress intensity factors  $A_1$  and  $A_2$  were calculated numerically using FEM and BEM. For the BEM determination, a special notch tip element was employed. Very good agreement could be achieved between the results of the two numerical techniques.

REFERENCES

- (1) Heuberger, A. (ed.) "Mikromechanik", Springer Verlag, Berlin, 1991.
- (2) Petersen, K.E., Proc. IEEE, Vol. 70, No. 5, 1982, pp. 420-457.
- (3) Stroh, A.N., Philos. Mag. 3, 1958, pp. 625-646.
- (4) Stroh, A.N., J. Math. Phys. 41, 1962, pp. 77-103.
- (5) Ting, T.C.T. and S.C. Chou, Int. J. Solids Structures 17, 1981, pp. 1057-1068.
- (6) Lin, K.Y. and Pin Tong, Int. J. Numer. Meth. Eng., Vol. 15, 1980, pp. 1343-1354.
- (7) Busch, M., Ph.D. dissertation, Universität Halle, 1990.

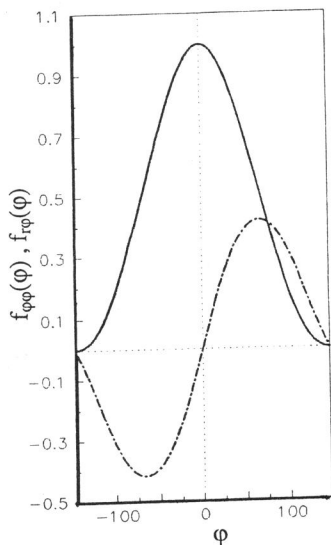


Figure 1:  $f_{\varphi\varphi_1}(\varphi)$  (solid line) and  $f_{r\varphi_1}(\varphi)$  (dashed line).

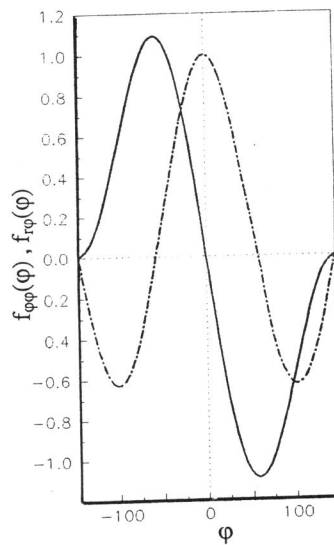


Figure 2:  $f_{\varphi\varphi_2}(\varphi)$  (solid line) and  $f_{r\varphi_2}(\varphi)$  (dashed line).

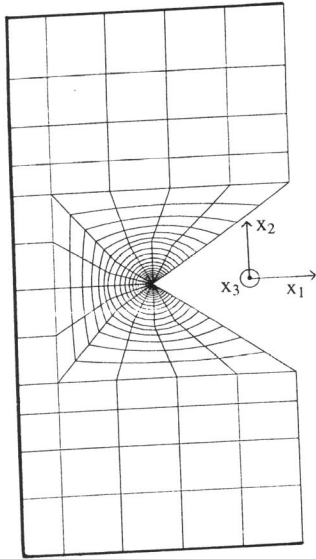


Figure 3: FEM mesh of a notched plate.

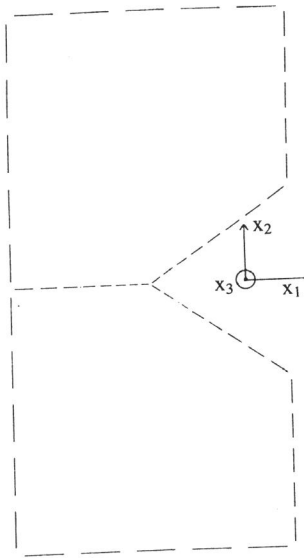


Figure 4: BEM mesh of a notched plate.

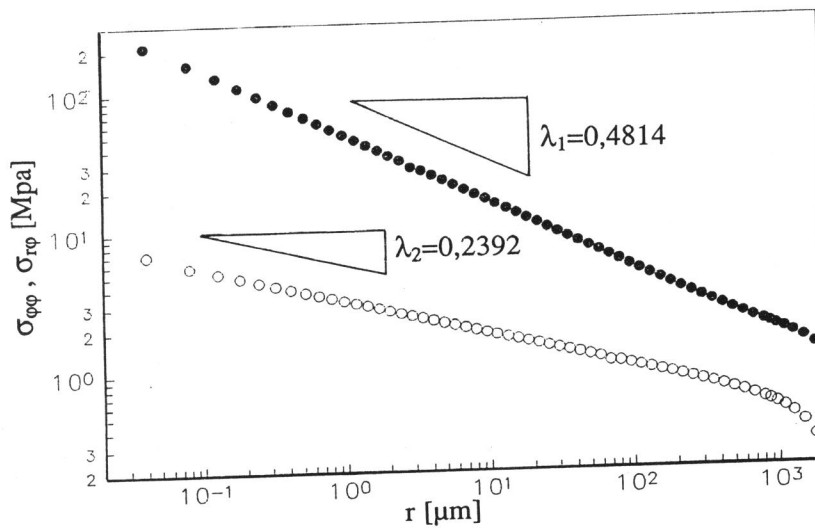


Figure 5: Nodal stresses  $\sigma_{\phi\phi}$  and  $\sigma_{r\phi}$  along along the ligament ahead of the notch tip.